Overview of ATLAS Forward Proton detectors for LHC Run 3 and plans for the HL-LHC

Maciej P. Lewicki[1]

E-Mail: maciej.lewicki@ifj.edu.pl

Institute of Nuclear Physics Polish Academy of Sciences, PL-31342 Krakow, Poland

Presented at the Low-x Workshop, Elba Island, Italy, September 27–October 1 2021 [2]

A key focus of the physics program at the LHC is the study of head-on proton-proton collisions. Among those, an important class of physics can be studied for cases where the protons narrowly miss one another and remain intact. In such cases, the electromagnetic fields surrounding the protons can interact producing high energy photon-photon collisions, for example. Alternatively, interactions mediated by the strong force can also result in intact forward scattered protons, providing probes of quantum chromodynamics. In order to aid identification and provide unique information about these rare interactions, instrumentation to detect and measure protons scattered through very small angles is installed in the beam-pipe far downstream of the interaction point. We describe the ATLAS Forward Proton 'Roman Pot' Detectors, including their performance to date and expectations for the upcoming LHC Run 3, covering Tracking and Time-of-Flight Detectors as well as the associated electronics, trigger, readout, detector control and data quality monitoring. The physics interest, beam optics and detector options for extension of the programme into the High-Luminosity LHC era are also discussed.

ATL-FWD-PROC-2021-002
17 December 2021

1 Introduction

The predictions of forward proton scattering arise in a diverse range of physics, including the hard [1, 2] and nonperturbative QCD [3], interactions at electroweak scale [4–7], and searches for physics beyond Standard Model [8–13]. Such events, usually called diffractive, involve an exchange of a colourless object between interacting protons, one or both of which may remain intact. Moreover, a *rapidity gap* will be present – an absence of particles produced into kinematic vicinity of the intact proton. Historically, rapidity gap is a standard experimental signature of a diffractive event, however, it is frequently outside the acceptance of detector, or is destroyed due to background, i.e. particles coming from *pile-up* – independent collisions happening in the same bunch crossing. An alternative method of identifying diffractive events is a direct measurement (*tagging*) of the scattered proton, which requires additional devices called *forward detectors* far downstream from the interaction point.

[1] on behalf of the ATLAS Collaboration

[2] Copyright 2021 CERN for the benefit of the ATLAS Collaboration. CC-BY-4.0 license.

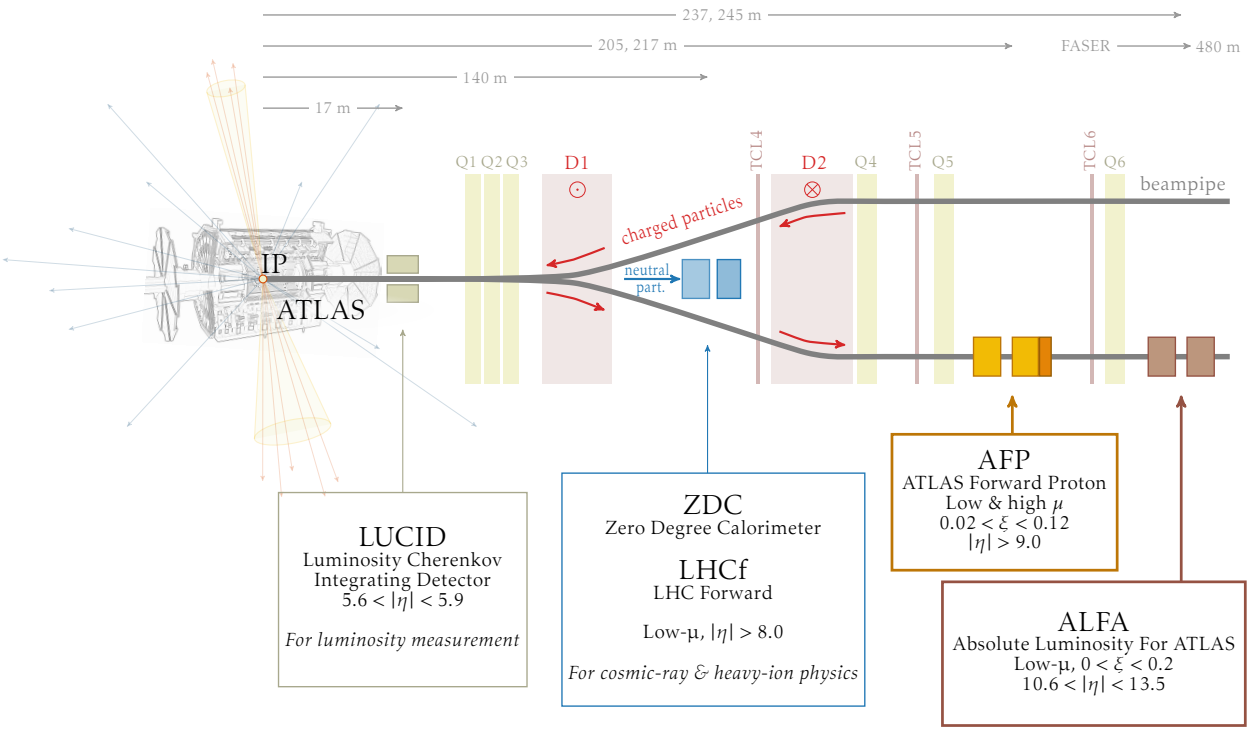

Figure 1: A diagram of Forward Detectors in the ATLAS experiment showing their placement with respect to beam lines and optical instrumentation: dipoles (D1, D2), quadrupoles (Q1–6) and collimators (TCL4–6).

2 Forward Spectrometers in ATLAS

ATLAS [14] forward spectrometers are a set of instruments housed in Roman Pot devices registering the protons scattered at very small angles. A proton scattered at the interaction point (IP) is deflected outside the beam envelope by dipole and quadrupole magnets of the LHC [15]. Its momentum can be determined by measuring points on its trajectory [16, 17]. The schematic layout of the forward spectrometers in ATLAS experiment with respect to the beam lines, optics instrumentation and other forward detectors is shown in Figure 1.

Absolute Luminosity For ATLAS (ALFA) performs measurements of soft diffraction and elastic scattering. It also provides an important input for Monte-Carlo generators, in particular, for modelling cosmic ray showers and simulation of the pile-up background. The ALFA spectrometer system consists of four vacuum-sealed spectrometers housed in Roman Pots, which are inserted vertically (top and bottom) onto the beam line. The NEAR and FAR stations are placed on each side of the ATLAS Interaction Point at 237 and 241/245[3] m respectively with the distance of the tracker's edge to the beam during normal operation at below 2 mm. Each station houses a multi-layer scintillating fibre (SciFi) consisting of two main detectors (10 layers of 64 fibers each) used for tracking, and 4 outer layers for the purpose of precise alignment. Achieved tracking resolution is approximately $\sigma = 30$ μm in both, vertical and horizontal direction. The read-out is performed by the Multi-Anode-Photo-Multipliers and dedicated scintillators provide the triggering capability. ALFA detectors require special running conditions of low pile-up as well as high β^* optics.

[3]FAR station was initially installed at 241 m (Run 1) and then moved to 245 m (Run 2) to improve the reconstruction of proton kinematics

ATLAS Forward Protons (AFP) spectrometer system consists of four Roman Pot stations. Their placement with respect to the beam lines is shown schematically in Figure 2. "NEAR" and "FAR" devices are placed at 205 m and 217 m on both sides of the IP and are inserted horizontally towards the beam. Each station houses four planes of 3D silicon pixel sensors [18–21] forming the silicon

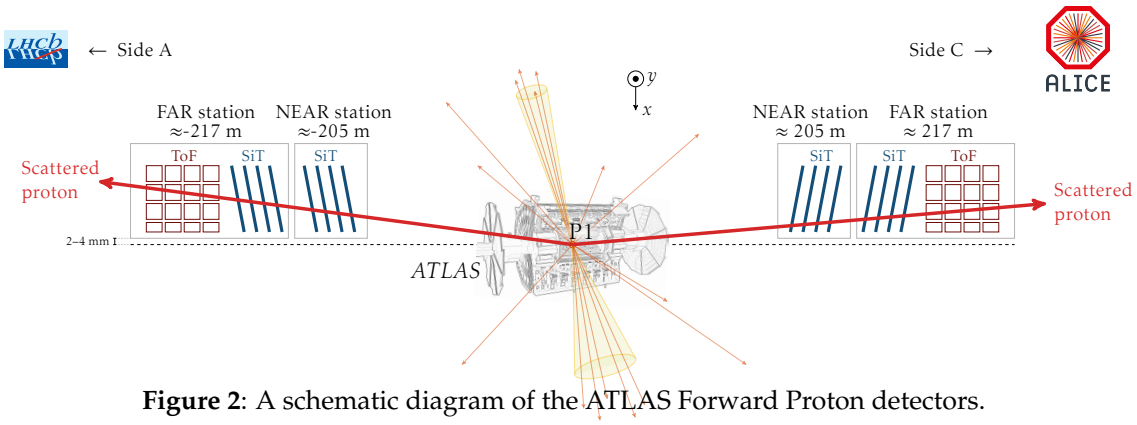

Figure 2: A schematic diagram of the ATLAS Forward Proton detectors.

tracker (SiT), which measures the trajectories of the scattered protons. The sensors have 336×80 pixels with 50×250 μm^2 area each, providing the combined spatial resolution of reconstructed proton tracks of 6 μm and 30 μm in x and y directions, respectively [22]. Optimal resolution in x coordinate is achieved with the sensors tilted by 14 degrees about the x-axis. The reconstruction

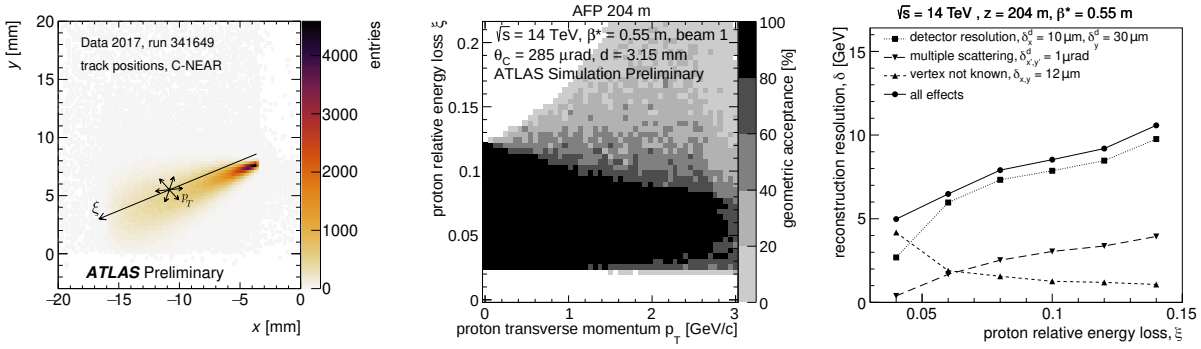

Figure 3: Left: example distribution of reconstructed track positions (x and y, transverse to the beam); the beam spot is approximately at (0,10) mm and deviations from this position are related to proton energy loss, as well as its transverse momentum (taken from [23]). Middle: Simulated geometric acceptance of the AFP detector as a function of the proton relative energy loss and its transverse momentum (from [16]). Right: AFP reconstruction resolution in dependence on proton relative energy loss ξ calculated accounting also for multiple scattering and unknown position of the collision vertex [16].

of position of protons traversing the AFP detectors (see Figure 3, left panel), in a known magnetic field, allows the estimation of proton energy and transverse momentum [24]. The main observable measured by the AFP is the proton fractional energy loss, defined as: $\xi = 1 - E_{\text{proton}}/E_{\text{beam}}$. The precision of unfolding proton kinematics based on the positions in AFP is directly affected by its spatial resolution. Figure 3 (right panel) illustrates how the resolution changes with proton relative energy loss (ξ). Additional effects that affect the resolution of proton energy reconstruction include the unknown position of the primary vertex and multiple scattering. The typical acceptance in ξ and p_{T} is illustrated in middle panel of Figure 3.

Time-Of-Flight (ToF) detectors are additional equipment present in Roman Pots at FAR stations. For processes in which protons are reconstructed on both sides of the IP, this allows rejection of background from pile-up by using the difference between the A and C-side ToF measurements to reconstruct the primary vertex position. The ToF detectors are based on Cherenkov radiation in quartz crystals, which leads to an excellent timing resolution. The performance of the ToF devices was measured for the data gathered in 2017 [25, 26] and obtained time resolution reaches values of 20 $\pm$ 4 ps and 26 $\pm$ 5 ps for sides A and C, respectively. Achieved time resolution translates to determination of primary vertex z-position with an accuracy of 5.5 $\pm$ 2.7 mm. Such level of precision allows for a substantial reduction of background in 'double-tag' events, as shown in Figure 4 (right). However, the observed efficiency of ToF reconstruction was very low (≈7%) due to fast PMT degradation during the data taking. Recently, new PMTs were installed and preliminary tests show readiness for use in upcoming data-taking campaigns of Run 3.

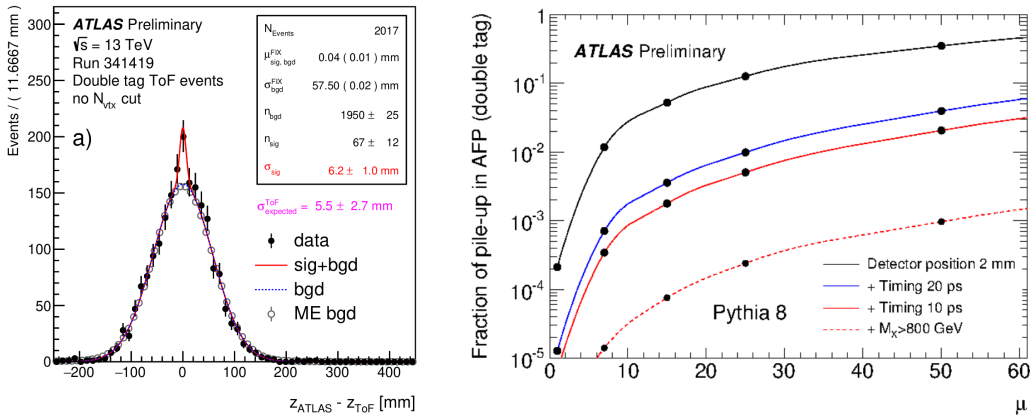

Figure 4: Left: Example distribution of $z_{\mathrm{ATLAS}} - z_{\mathrm{ToF}}$ measured in events with ToF signals on both sides of the interaction region, where z_{ATLAS} stands for vertex z-positions reconstructed as primary ones by ATLAS (taken from [27]). Right: A simulation of the fraction of pile-up events present in the data sample with a double AFP tag shown in dependence of the mean pile-up and for various timing resolutions (taken from Ref. [16]).

AFP global alignment is performed by comparing the proton relative energy loss measured in the AFP ξ_{AFP} with a corresponding value calculated based on the kinematics of produced lepton pair ξ_{ll}:

$$\xi_{\mathrm{AFP}} = 1 - \frac{E_{\mathrm{proton}}}{E_{\mathrm{beam}}}, \qquad \xi_{ll}^{\mathrm{A/C}} = \frac{m_{ll} e^{(+/-)y_{ll}}}{\sqrt{s}} \tag{2.1}$$

The AFP alignment parameters are adjusted in such a way that the maximum of the distribution of $\xi_{\mathrm{AFP}} - \xi_{\mu\mu}$ is at zero. Figure 5 illustrates the differences between projected track x position based on lepton kinematics and the one measured by AFP, before and after alignment correction. A valuable advantage of such method is a low and well-modelled background, which allows achieving alignment precision currently quoted at 300 μm. Continued studies of data and simulation show promise that this value can be further improved.

AFP track reconstruction efficiency is calculated using a so called 'tag-and-probe' method. The efficiency is defined as the ratio of events in which the track is recorded in one station (*tag*) and not in the other (*probe*) to the total number of events with tagged tracks. Measured track reconstruction efficiency during the 2017 data taking campaigns are shown in Figure 6. NEAR stations record efficiency over 98% for all studied datasets. A possible effect that might contribute to lower

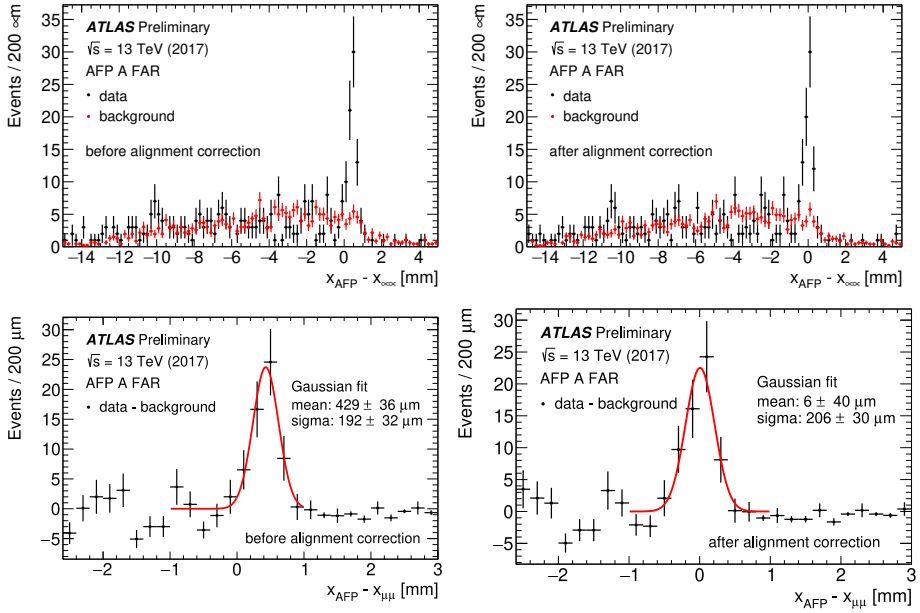

Figure 5: The distribution of differences between measured track position x_{AFP} and position expected based on dilepton system kinematics $x_{\mu\mu}$, compared with the background model based on event-mixing. The figures on the right show the same as those on the left after correcting the x coordinates of all events by the alignment constant (taken from Ref. [28]).

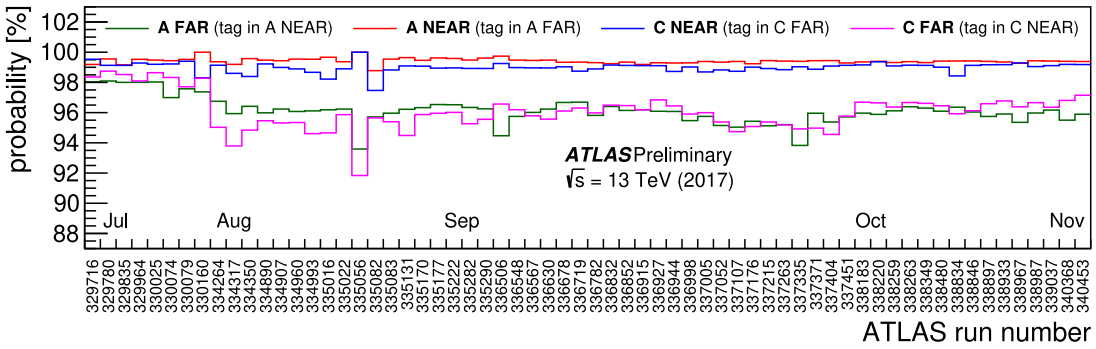

Figure 6: Track reconstruction efficiencies recorded in high-luminosity runs during 2017 data-taking (taken from Ref. [28]).

efficiencies of FAR stations (95% – 98%) is the radiation degradation of the silicon tracker, as the FAR stations are inserted slightly closer (<1 mm) to the beam and are more exposed to the beam halo. However, lower efficiencies observed in FAR stations, are also a natural consequence of the 'tag-and-probe' method used in this analysis, as the downstream stations are additionally affected by the showers created by interactions with detector material in the upstream station. The existence of showers is evident when examining the long non-Poisson tail in hit multiplicity per plane, which is higher for each consecutive pixel layer. Additionally, each consecutive plane registers on average higher number of hits (pixels that record a signal exceeding a threshold) and higher charge deposits, which is also expected under the presence of cascades created by interactions with SiT and Roman Pot floor. Both effects are illustrated in Figure 7.

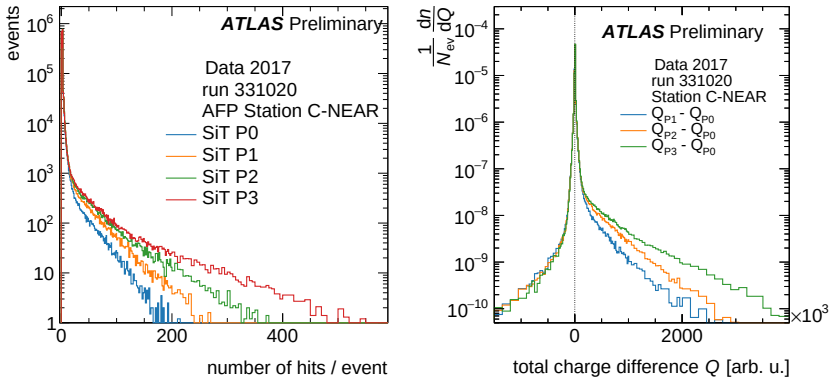

Figure 7: Distribution of the number of hits per event (left) and the difference of recorded charge for each of silicon planes in C-NEAR station (right). Secondary interactions with detector material result in higher number of hits and higher recorded charge for consecutive SiT planes (taken from Ref. [23]).

3 Status and plans for Run 3

No major changes between Run 2 and Run 3 are planned in terms of detector technology, although numerous hardware and software updates were implemented. The AFP tracker system was equipped with newly produced tracking modules and new heat exchangers were installed to improve cooling capabilities. Due to the repeated failures of MCP-PMTs in vacuum, the AFP ToF detector was redesigned with MCP-PMTs placed out of the detector secondary vacuum. The newly designed construction of the R2D2 based MCP-PMT back-end electronics was developed, successfully tested and used in the construction of the new ToF device. Additionally, a set of new, glue-less LQBars was installed, as well as picoTDC, single-channel pre-amplifiers, modified trigger and pulser modules. Updated systems were exposed to proton beams at DESY and CERN SPS and successfully underwent performance tests.

The design of ALFA trackers remained unchanged as well and minor hardware updates include improvements to the cooling system and exchange of the readout electronics (due to radiation damage). All subsystems of both AFP and ALFA spectrometers are installed in LHC tunnels and are fully prepared for data-taking campaigns starting in 2022.

Similarly, good progress is observed in development of software and simulation necessary for physics analyses of forward protons in ATLAS. Advances in studies of tracker performance and beam optics, as well as improvements in precision of detector alignment allow delivering a high-accuracy proton physics object to ATLAS. The properties of forward protons reconstructed with AFP and ALFA are used in several analyses across different working groups in ATLAS. A dedicated task force (Proton Combined Performance group) leads efforts to improve understanding of the proton object, including assessment of tracker efficiency or susceptibility to physical conditions, leading to a possible reduction of systematic uncertainties. Additionally, an ongoing work aiming at implementation of full GEANT4 simulation will allow to better understand possible effects related to detector geometry, alignment or interactions with detector material. Progresses in areas listed above contribute to advances with physics analysis, which are discussed in more detail in Section 4.

	Run 2	**Run 3 plans (requests)**
beam and optics	$\sqrt{s} = 13$ TeV, $\beta^* = 0.3$ m, 0.4 m	$\sqrt{s} = 13$ TeV, $0.2 < \beta^* < 1.1$ m
AFP setup	one-arm (2016), two-arms (2017)	two-arms + TOF
Standard runs	$\langle\mu\rangle \approx 35$, int. lumi. 46.9 fb^{-1}	$\langle\mu\rangle < 60$, $\mathcal{O}(500$ fb$^{-1})$
Special runs at $\mu \approx 0$ (soft diffraction)	int. lumi.: ≈ 100 nb^{-1}	$\mathcal{O}(100$ nb$^{-1})$
Special runs at $0.3 \lesssim \mu \lesssim 1$ (low p_T jets)	int. lumi.: ≈ 1.15 pb^{-1}	$\mathcal{O}(1$ pb$^{-1})$
Special runs at $\mu \approx 2$ (EW, hard diffr., SD $t\bar{t}$)	int. lumi.: ≈ 150 pb^{-1}	$\mathcal{O}(100$ pb$^{-1})$

Table 1: Comparison of most important properties of data taken by AFP in Run 2 and requests for Run 3 data taking.

	Run 2	**Run 3 plans (requests)**
collision energy	$\sqrt{s}$=13 TeV	$\sqrt{s} \geq 13.5$ TeV,
beam conditions	β^*=90 m, 2.5 km	β^*= 3, 6 km and/or β^*_x= 3 km, β^*_y= 6 km
	$\langle\mu\rangle \approx 35$, $\langle\mu\rangle \approx 0$	only at $\langle\mu\rangle \approx 0$

Table 2: Comparison of most important properties of data taken by ALFA in Run 2 and possible plans for Run 3

4 Recent ATLAS physics results with forward proton tag

4.1 First physics analysis with AFP proton tag

The analysis of the rich data collected by ATLAS Forward Protons detector is ongoing and recently the results on semi-exclusive dilepton production associated with forward proton scattering were published [29], delivering the cross-sections measurements for $pp \to p(\gamma\gamma \to l\bar{l})pp^*$ processes. Modelling of photon fusion in proton-proton interactions is poorly constrained, particularly at high $\gamma\gamma$ invariant masses. Direct proton measurement allows for a strong background suppression by means of kinematic matching of tagged forward protons and leptons measured in the central detector. The fractional proton energy loss measured in AFP, ξ_{AFP}, can be compared against the value of $\xi_{l\bar{l}}$ that can be derived from dilepton system kinematics as defined in Eq. (2.1). With the criterium of $|\xi_{\text{AFP}} - \xi_{l\bar{l}}| < 0.005$ a total of 57 and 123 candidates in the $ee + p$ and $\mu\mu + p$ final states were observed. With a background rejection on the level of ≈85% and signal acceptance on the level of ≈95% this corresponds to statistical significance of over 5σ in each production channel, thus providing a direct evidence of forward proton scattering in association with electron and muon pairs produced via photon fusion. Table 3 summarizes obtained cross sections for these processes in the detector fiducial region compared with the relevant theoretical predictions. Figure 8 shows a distribution of measured $\xi_{\text{AFP}} - \xi_{l\bar{l}}$ for both sides A and C together with predictions associated with various production channels.

4.2 Single diffraction results with ALFA proton tag

In a recent publication [30], a dedicated sample of low-luminosity (mean pile-up $\langle\mu\rangle < 0.08$) proton-proton collision data at $\sqrt{s}$ = 8 TeV is used to study of the dynamics of the inclusive single-

$\sigma_{\text{HERWIG+LPAIR}} \times S_{\text{surv}}$	$\sigma^{\text{fid.}}_{ee+p}$ (fb)	$\sigma^{\text{fid.}}_{\mu\mu+p}$ (fb)
$S_{\text{surv}} = 1$	15.5 ± 1.2	13.5 ± 1.1
S_{surv} using EPJC 76 (2016) 9 PLB 741 (2015) 66	10.9 ± 0.8	9.4 ± 0.7
SUPERCHIC	12.2 ± 0.9	10.4 ± 0.7
Measurement	$\mathbf{11.0 \pm 2.9}$	$\mathbf{7.2 \pm 1.8}$

Table 3: Summary of model predictions on cross-sections for diffractive processes of di-lepton production compared with AFP measurements.

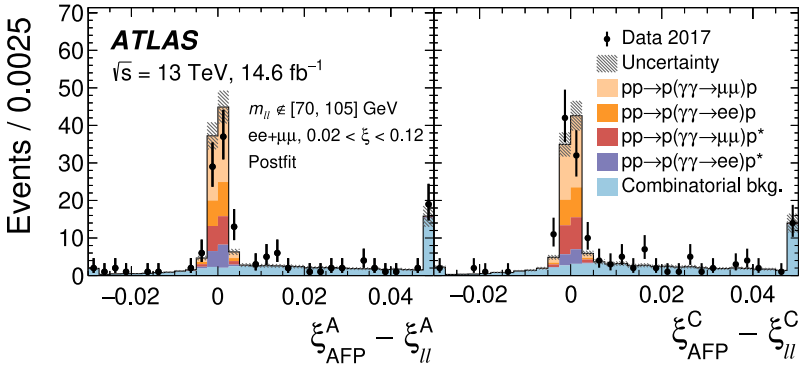

Figure 8: Distributions of $\xi_{\text{AFP}} - \xi_{l\bar{l}}$ with $\xi_{l\bar{l}}$ and ξ_{AFP} both in range [0.02, 0.12]. Black points with error bars illustrate data and its statistical uncertainty and coloured stacks represent model predictions for various processes contributing to the measured signal (p* denotes dissociated proton) with hatched area indicating their combined uncertainty (plots from Ref. [29]).

diffractive dissociation process $p\,p \to X\,p$. Improving on previous related analyses, besides measurements of charged particles from the dissociated system X performed by the central ATLAS detector components, the ALFA forward spectrometer provides reconstruction of the final-state intact protons. The differential cross sections are measured as a function of the fractional proton energy loss ($-4.0 < \log_{10}\xi < -1.6$), the squared four-momentum transfer ($0.016 < |t| < 0.43\,\text{GeV}^2$), and the size of the rapidity gap $\Delta\eta$. The total cross section integrated across the fiducial range is shown in Table 4 with additional information on predictions of relevant theoretical models. As

Distribution	$\sigma^{\text{fiducial}(\xi,t)}_{\text{SD}}$ [mb]	$\sigma^{t-\text{extrap}}_{\text{SD}}$ [mb]
PYTHIA8 A2 (Schuler-Sjöstrand)	3.69	4.35
PYTHIA8 A3 (Donnachie-Landshoff)	2.52	2.98
HERWIG7	4.96	6.11
Measurement	$\mathbf{1.59 \pm 0.13}$	$\mathbf{1.88 \pm 0.15}$

Table 4: Summary of model predictions on cross-sections for single soft diffraction compared with the measurements by ALFA.

shown in Figure 9 the data are consistent with an exponential t dependence, $\mathrm{d}\sigma/\mathrm{d}t \propto e^{Bt}$ with slope parameter $B = 7.65 \pm 0.34\,\text{GeV}^{-2}$. Interpreted in the framework of triple Regge phenomenology, the ξ dependence leads to a Pomeron intercept of $\alpha(0) = 1.07 \pm 0.09$.

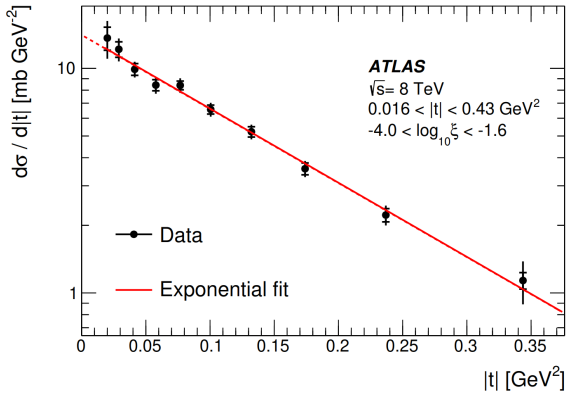

Figure 9: The differential cross section as a function of $|t|$ with statistical and total uncertainties represented by inner and outer error bars, respectively. Red line shows fitted exponential function (plot taken from Ref. [30]).

5 HL-LHC with AFP perspectives

Predictions of forward proton scattering appear in a diverse range of topics, providing strong motivation for continuation of experimental efforts. Diffractive processes were identified as a potential mechanism of top quark [3], as well as exclusive Higgs boson production [8, 9]. Additionally, measurements of intact protons may provide a valuable input in the studies of two-photon processes in the context of SM electro-weak interactions [6, 7], but also in high-mass sector beyond-SM [10]. Extending the potential of new physics discoveries, a capability of direct proton tagging may be an important tool in the searches of sleptons and dark matter [12, 13], as well as axion-like particles [11]. An important input to understanding the QCD sector of the SM and beyond may be also provided by novel studies of exclusive diffractive events [1, 2].

While the rich physics opportunities open up with the capability of forward proton tagging, a number of challenges remain that keep the presence of AFP detectors in ATLAS operation after Long Shutdown 3 under discussion. The HL-LHC will feature a novel beamline that includes crab cavities, collimators and magnets at new positions and different settings. The beam instrumentation properties planned for Run 4 place Point 1 optics at a disadvantage comparing to conditions in Runs 2 and 3. The RP acceptance might be limited due to placement of beam optics devices (collimators, cavities), but more importantly, the beam crossing angle of $\phi = 180^\circ$ renders the trajectories of diffractive protons closer to the beam, which in turn impairs the resolution of energy measurement. The second major challenge is the rejection of background under the conditions of mean pile up at $\langle\mu\rangle \approx 200$. A distinction of individual vertices would only be reliable with a sub-10 ps precision of ToF detectors (Silicon/LGAD/Cherenkov technology) and additional timing devices in the central ATLAS detector. Similarly, novel solutions will be required in the area of data acquisition and analysis due to high event rates and consequently large data volumes. Parallel to technological challenges, an important practical issue is the acquisition and sustainability of manpower and resources for a time period of over 20 years.

6 Summary

The ATLAS Forward Proton spectrometers, ALFA and AFP, provide a capability of forward proton tagging and measuring its kinematics, thus delivering an important data in the studies of diffractive physics. Both detector systems recorded rich datasets of standard and special, low-luminosity

conditions during LHC Run 2. The analyses of collected data are ongoing and active efforts are directed into improvement of data quality, including the accuracy of detector alignment or the estimation of trackers efficiencies. First experimental results on dilepton production with AFP tag were recently published and many more measurements of diffractive and exclusive events from Run 2 data will come in a near future. Similarly, first results on single diffraction with a tag in ALFA were published in 2020 and more analyses on diffractive and elastic processes are ongoing.

Both AFP and ALFA spectrometers underwent hardware improvements and, after successful tests with proton beams at DESY and SPS, were installed in the LHC tunnel and are ready for further tests preparing for Run 3 data-taking campaigns. The collection of physics data is expected to begin in Spring 2022 and in the course of next four years it is expected that the AFP will collect an order of magnitude more data for studies of diffractive physics.

The continuation of forward physics programmes in the HL-LHC era is currently under discussion within ATLAS. While a wide range of physics topics would benefit from forward proton tagging, a number of experimental challenges remain. The constraints on preferred detector localization and utilized technology are being discussed and corresponding feasibility studies are performed in parallel. Were the AFP to take data in Run 4, an optimization of beam optics must be considered in order to enhance the spectrometer acceptance.

Acknowledgements

This work was partially supported by the Polish National Science Centre grant: 2019/34/E/ST2/00393.

References

[1] M. Trzebinski, R. Staszewski, J. Chwastowski, Eur. Phys. J. C (2015) 75: 320

[2] V. P. Goncalves et al., Phys. Rev. D 102, 074014 (2020).

[3] James Howarth, arXiv:2008.04249.

[4] CMS and TOTEM Collaborations, JHEP 07 (2018) 153.

[5] ATLAS Collaboration, Phys. Rev. Lett. 125, 261801 (2020).

[6] S. Tizchang, S. M. Etesami, JHEP 07 (2020) 191.

[7] C. Baldenegro et. al., JHEP 12 (2020) 165.

[8] B. E. Cox, F. K. Loebinger, A. D. Pilkington, JHEP 0710:090, 2007.

[9] S. Heinemeyer et al., Eur.Phys.J.C53:231-256,2008.

[10] S. Fichet et al., Phys. Rev. D 89, 114004.

[11] C. Baldenegro et al., JHEP 06 (2018) 131.

[12] L. Beresford, J. Liu, Phys. Rev. Lett. 123, 141801 (2019)

[13] L.A. Harland-Lang et al., JHEP 04 (2019) 10

[14] ATLAS Collaboration, JINST 3 (2008) S08003.

[15] L. Evans and P. Bryant, JINST 3 (2008) S08001.

[16] ATLAS Collaboration, tech. rep. CERN-LHCC-2015-009, 2015.

[17] M. Trzebiński, Proc.SPIE Int.Soc.Opt.Eng. 9290 (2014) 929026

[18] J. Lange, E. Cavallaro, S. Grinstein and I. López Paz, JINST 10 (2015) C03031.

[19] J. Lange et al., JINST 529 11 (2016) P09005.

[20] M. Garcia-Sciveres et al., Nucl. Instrum. Meth. A 636 531 (2011) S155.

[21] V. Zivkovic et al., Journal of Instrumentation 7 (2012) C02050.

[22] S. Grinstein et al., JINST 12 (2017) C01086.

[23] M. P. Lewicki, PoS LHCP2021 (2021) 241, pos.sissa.it/397/241

[24] M. Trzebiński, R. Staszewski, J. Chwastowski, ISRN High Energy Phys. 2012 (2012) 491460

[25] T. Sykora, 540 Journal of Instrumentation 15 (2020) C10004.

[26] K. Cerny, PoS Vertex2019 (2020) 055.

[27] K. Cerny, ATL-FWD-PUB-2021-002, cds.cern.ch/record/2749821/

[28] R. Staszewski, J. Liu, ATL-COM-FWD-2020-008, cds.cern.ch/record/2723730

[29] ATLAS Collaboration, Phys. Rev. Lett. 125 (2020) 261801

[30] ATLAS Collaboration, JHEP 02 (2020) 042, JHEP 10 (2020) 182 (erratum)